Photoionization and Rydberg states of N_2

Carolyn Duzy* and R. Stephen Berry

Department of Chemistry and The James Franck Institute, The University of Chicago, Chicago, Illinois 60637
(Received 16 September 1975)

The frequencies and intensities of transitions to Rydberg levels, the direct photoionization cross section, and the angular distribution of photoelectrons of N_2 have been calculated for processes associated with $N_2^+(X\,^2\Sigma_g^+)$ and $N_2^+(A\,^2\Pi_u)$. The theoretical model is based on a Hartree–Fock wavefunction for the ground state of N_2, and excited state wavefunctions derived from an irreducible-tensorial one-center representation of the effective potential of the N_2^+ core. The calculations were carried out for several internuclear distances, especially to try to interpret the dependence of the angular distribution on the final vibrational state.

I. INTRODUCTION

The nitrogen molecule absorbs radiation of wavelength 79.59 nm (15.58 eV) or less to produce N_2^+ in its ground $X\,^2\Sigma_g^+$ electronic state, or radiation of wavelength 74.27 nm (16.69 eV) or less, to produce N_2^+ in its first excited $A\,^2\Pi_u$ electronic state. Two optically allowed Rydberg series converge to the $X\,^2\Sigma_g^+$ limit, the Worley–Jenkins series[1] which (apart from the first member) is now known[2–4] to be the $np\pi_u\,^1\Pi_u$ series, and the $np\sigma_u\,^1\Sigma_u^+$ series identified by Carroll and Yoshino.[3] Two series, the $ns\sigma_g\,^1\Pi_u$ series known as Worley's Third[5] and the $ns\sigma_g\,^3\Pi_u$ series of Ogawa and Tanaka[6] definitely lead to the $A\,^2\Pi_u$ state of the ion. Four other series found by Ogawa[7] probably lead to the $A\,^2\Pi$ state also.

The molecule has the closed-shell configuration $(1\sigma_g)^2(1\sigma_u)^2(2\sigma_g)^2(2\sigma_u)^2(1\pi_u)^4(3\sigma_g)^2$ in its ground state. The Worley–Jenkins and Carroll–Yoshino series and the first ionization limit arise from excitation of an electron from the $3\sigma_g$ orbital. Worley's Third series, and its companions, and the second ionization limit arise from excitation of an electron from the $1\pi_u$ inner shell lying slightly below the $3\sigma_g$.

The cross section for direct photoionization of N_2 in the region of the $X\,^2\Sigma_g^+$ and $A\,^2\Pi_u$ states of the ion has been measured by Cook and Metzger,[8] by Cook and Ogawa,[9] and very recently by Samson.[10] Carlson and Jonas determined the angular distribution of photoelectrons in this energy range,[11] and find a dependence of this distribution on the final vibrational quantum number for production of the $^2\Sigma_g^+$ state of N_2^+, which comes as a bit of a surprise. No such dependence was found for production of the $A\,^2\Pi_u$ state of N_2. Berkowitz and Chupka have examined the photoionization spectrum of N_2 cold (78 K) with a resolution of 0.012 nm, and have distinguished both the continuous background and a great many peaks associated with the photoexcitation of autoionizing levels.[12] More recently, Dehmer and Chupka have obtained a photoionization spectrum for N_2 with a resolution of 0.0017 nm over the range 79.7–77.5 nm, and 0.0035 nm from 77.5 to 71.3 nm.[13] This resolution is high enough to allow observation of rotational splittings in some of the photoionization peaks associated with autoionizing levels.

We have carried out a theoretical investigation of the photoionization of N_2, consisting of two parts. In this part, we discuss the energies and intensities of the Rydberg levels and the cross sections and angular distributions of photoelectrons associated with direct photoionization—in other words, the direct processes. In the second paper, we present our results concerning the mechanisms, rates and lines shapes for autoionization. The purposes of our study were manifold: the evaluation of the intensities for excitation and ionization, the interpretation of the puzzling angular distribution, the inference of the relative importance of vibronic and electron correlation mechanisms in the autoionization process and an inquiry into the possible differentiation of the two mechanisms on the basis of the shapes of their autoionization "lines." (At present, this turns out to be impossible at least, because of incompletely resolved rotational structure in the "lines," and perhaps because of lifetime broadening as well.) Underlying all of these is, of course, our continuing interest in the development of a computational method capable of yielding usefully accurate representations of the photoionization of molecules more complicated than H_2.

The method we have developed is similar in spirit to the one used to treat N_2 by Schneider and Berry[14] in that the optical transition is treated as a one-electron excitation and the initial and final states of the "active" electron are based on solutions of one-electron Schrödinger equations. The method differs from that used by Schneider and Berry in that the method used here does not rely on empirical data; Schneider and Berry used extrapolations of experimentally determined energies of Rydberg states to fix the phase shifts for their continuum functions, while we compute these phase shifts *ab initio*. The method is also similar in spirit to the approaches of Berry and Nielsen[15] and Ritchie[16] in that the effective potential for the active electron in Rydberg and continuum states is expanded as a series of irreducible tensors. This turns out to be far more accurate than a simple multipole expansion, yet only a little more difficult to execute.

In order to study the dependence of the angular distribution of photoelectrons on the final vibrational state, we of course had to evaluate all our electronic transition processes at various values of the internuclear distance R. Our budget permitted us to use three values of R in calculating direct photoionization, and

four values of R for autoionization, which appear to be sufficient to show the principal features of the R dependence of the transition amplitudes.

II. THEORY AND METHOD

We seek to compute the term values and electric-dipole transition probabilities of the optically accessible Rydberg states, and the photoionization cross section and angular distribution parameter as functions of energy.

The photoionization cross section in the electric dipole approximation is[17]

$$\sigma = (8\pi^3 e^2 \nu/3c)\ |\langle f|\mathbf{r}\cdot\mathbf{z}|i\rangle|^2, \tag{1}$$

when ν in the frequency of the radiation, f and i denote final and initial states of the entire system, $\mathbf{z}$ denotes the polarization vector of the light and $\mathbf{r}$ is the coordinate vector (set) of the particles responding to the applied electromagnetic field, which, for us, are essentially the coordinates of the one active electron.

The angular distribution of photoelectrons emitted from an isotropic ensemble by a linearly polarized one-photon, electric-dipole process is given by[18,19]

$$d\sigma/d\theta = \tilde{\alpha} + \tilde{\beta}\cos^2\theta = (\sigma/4\pi)[1 + \beta P_2(\cos\theta)], \tag{2}$$

so

$$\beta = 2/[3(\tilde{\alpha}/\tilde{\beta}) + 1];$$

θ is the observation angle relative to the polarization axis. For measurements made with unpolarized light, the direction of light propagation becomes the reference axis with respect to which θ', the angle of the momentum vector of the outgoing electron, is measured[19]:

$$d\sigma/d\theta' = A[1 + B\sin^2\theta'],$$

and

$$B = 4\beta/(3 + 2\beta). \tag{3}$$

The general matrix element appearing in Eq. (1) and the parameters $\tilde{\sigma}$ and $\tilde{\beta}$, σ and β or A and B of Eqs. (2) and (3) are all most naturally expressed in terms of the electric dipole matrix elements $d_{\ell m}$ evaluated in a molecule-fixed coordinate system:

$$d_{\ell m} = \iint dR\, d\mathbf{r}\psi^*_{k\ell m}(\mathbf{r}, R)\chi_f^*(R) r\, Y_{\ell m''}\psi_i(\mathbf{r}, R)\chi_i(R)C(R). \tag{4}$$

Here R is the internuclear distance, r is the position of the active electron, m'' is the difference between the azimuthal quantum numbers of the outgoing and initial states; $\psi_{k\ell m}(r, R)$ is the final-state continuum wavefunction of the outgoing electron with angular momentum quantum numbers ℓ, m; χ_f is the final-state vibrational wavefunctions of the N_2^+ core, $\psi_i(r, R)$ is the initial orbital ($3\sigma_g$ or $1\pi_u$ in our example) of the active electron, $\chi_i(R)$ is the initial vibrational wavefunction of the neutral N_2, and $C(R)$ is the overlap integral (a function of R) of all the initially occupied orbitals of N_2 (except ψ_i) with the occupied orbitals of N_2^+.

Following the method of Tully, Berry, and Dalton[20] for ionization of an ensemble of randomly oriented molecules whose rotational motion can be neglected, we obtain the angular distribution parameters:

for $N_2^+(X^2\Sigma_g^+) + p$-wave electron,

$$\tilde{\alpha} = \frac{4\pi^2 e^2 \nu}{15c}\ [|d_{10}|^2 + |d_{11}|^2 - 2\,\mathrm{Re}(d_{10}d_{11})], \tag{5a}$$

$$\tilde{\beta} = \frac{4\pi^2 e^2 \nu}{15c}\ [2|d_{10}|^2 + 7|d_{11}|^2 + 6\,\mathrm{Re}(d_{10}d_{11})]. \tag{5b}$$

In terms of the phase shifts δ_{10} and δ_{11} of the $p\sigma$ and $p\pi$ partial waves,[14] we replace $\mathrm{Re}(d_{10}d_{11})$ with $|d_{10}|\,|d_{11}|\cos(\delta_{10} - \delta_{11})$.

For $N_2^+(A^2\Pi_u) + s$- and d-wave electron, we have

$$\tilde{\alpha} = \frac{4\pi^2 e^2 \nu}{9c}\ [|d_{00}|^2 + (\tfrac{8}{7})|d_{20}|^2 + (\tfrac{6}{7})|d_{2-1}|^2 + (\tfrac{6}{7})|d_{2-2}|^2 + (\sqrt{5}/5)\mathrm{Re}(d_{00}d_{20}) + (\sqrt{15}/5)\mathrm{Re}(d_{00}d_{2-1}) + (\sqrt{30}/5)\mathrm{Re}(d_{00}d_{2-2}) + (\sqrt{3}/7)\mathrm{Re}(d_{20}d_{2-1}) - (2\sqrt{6}/7)\mathrm{Re}(d_{20}d_{2-2}) - (3\sqrt{2}/7)\mathrm{Re}(d_{2-1}d_{2-2})], \tag{6a}$$

$$\tilde{\beta} = \frac{4\pi^2 e^2 \nu}{9c}\ [(\tfrac{3}{7})|d_{20}|^2 - (\tfrac{3}{7})|d_{2-1}|^2 - (\tfrac{3}{7})|d_{2-2}|^2 + (3\sqrt{5}/5)\mathrm{Re}(d_{00}d_{20}) + (3\sqrt{15}/5)\mathrm{Re}(d_{00}d_{2-1}) + (3\sqrt{30}/5)\mathrm{Re}(d_{00}d_{2-2}) + (3\sqrt{3}/7)\mathrm{Re}(d_{20}d_{2-1}) - (6\sqrt{6}/7)\mathrm{Re}(d_{20}d_{2-2}) - (9\sqrt{2}/7)\mathrm{Re}(d_{2-1}d_{2-2})]. \tag{6b}$$

We take the basic wavefunctions $\Psi(r_1, \ldots, r_n, R)$ of the molecule to be products of electronic wavefunctions $\Phi(r_1, \ldots, r_n, R)$ and vibrational functions $\chi(R)$:

$$\Psi = \Phi\chi, \tag{7}$$

where the electronic function Φ is a solution of the molecular Born-Oppenheimer Hamiltonian $\mathcal{H}_e(r_1, \ldots, r_n, R)$. In the present treatment, we assume that the molecules form an isotropic ensemble and that their rotational motion can be neglected.

We obtained the vibrational wavefunctions $\chi(R)$ for the molecular ground state ($X^1\Sigma_g^+$) and the ground ($X^2\Sigma_g^+$) and first excited doublet ($A^2\Pi_u$) states of the N_2^+ ion by numerical integration of the corresponding one-dimensional Schrödinger equations for a vibrator in the state $J = 0$. The potentials $V(R)$ were those given by Gilmore.[21] Numerov's method[22] was used to carry out the computation. The eigenvalues that were also computed this way agreed with those obtained from the spectroscopic constants to within about 2%. Eigenvalues and eigenfunctions were determined by inward and outward integration.

As in all calculations of molecular transition probabilities, the nub of the problem is in obtaining the

electronic wavefunctions. Our method introduces three simplifying approximations beyond the Hartree–Fock and Born–Oppenheimer approximations:

(1) The effects of exchange on the active electron are represented by an effective local potential V_E in the manner proposed by Slater,[23] but with the numerical coefficient of the electron density, $\rho(k, R)$ taken to be that given by Tong and Sham[24]:

$$V_E(k, R) = [3\rho(k, R)/\pi]^{1/3}. \tag{8}$$

This method of representing exchange was employed by Berry and Nielson[15,25] in their study of Rydberg states and autoionization rates in H_2;

(2) The outgoing electron is assigned to a *single* angular-momentum partial wave, in the case of ionization; for Rydberg states, the excited-states orbitals are superpositions of p and f functions for the series converging to the $^2\Sigma^+$ limit and superpositions of s, d, and g functions for the series converging to the $^2\Pi_u$ limit. This procedure is thus more limited and less accurate in principle than the method of the most recent calculations of Ritchie, in which continuum functions are represented as mixtures of partial waves[26,27];

(3) The one-electron functions for the excited states were obtained in the "frozen-core" approximation, in which the molecular core is described by the wavefunction for the free molecule-ion, N_2^+, in its appropriate electronic state in our example.

The method we employed is this. The wavefunctions we selected to represent the ground state of the neutral N_2 molecule and N_2^+ in its $^2\Sigma_g^+$ and $^2\Pi_u$ states were those given by Cade, Sales, and Wahl (CSW).[28] These are single-configuration, Hartree–Fock functions, and are available at internuclear distances from 1.8 to 2.6 bohr, which allowed us to carry out our calculations for internuclear distances of 1.8, 2.113, 2.3, and 2.6 bohr. (The computed equilibrium distance of the N_2 ground state is 2.113 bohr, reasonably close to the experimental value of 2.074.) The matrix elements connecting the $X^1\Sigma_g^+$ state of N_2 with the bound excited states and the ionized states all contain the factor

$$C(R) = \int \Psi_f^*(\mathbf{r}_i, \ldots, \mathbf{r}_{n-1})\Psi_i(r_i, \ldots, r_{n-1})d\mathbf{r}_i \ldots d\mathbf{r}_{n-1}, \tag{9}$$

connecting the initial function Ψ_i and the final function Ψ_f of the $n-1$ inactive electrons. The functions $C(R)$ were computed from the CSW orbitals.

The CSW wavefunctions for N_2^+ were evaluated and transformed into numerical tabular form (on magnetic tape) in spherical polar coordinates with origin at the center of mass and charge of the molecule. The corresponding electron density $\rho(\mathbf{k}, R)$ was computed and then *expanded in irreducible tensorial components*. Thus we have, for linear molecules in general,

$$\rho(\mathbf{r}, R) = \sum_J \rho_J(r, R)Y_{J0}(\theta), \tag{10}$$

$$\rho_J(r, R) = \iint \rho(\mathbf{r}, R)Y_{J0}\sin\theta\, d\theta\, d\varphi. \tag{11}$$

The potential can then be constructed in a very convenient form

$$V(r, R) = \sum_{J=0}^{\infty}(V_{JC} + V_{JE}), \tag{12}$$

where V_{0C}, V_{2C}, etc., are the monopole, quadrupole, and higher tensorial components of the coulomb potential and V_{0E}, V_{2E}, etc., are the corresponding components of the effective local potential approximating the exchange potential. The Coulombic monopole potential is

$$V_{0C}(r, R) = \frac{1}{r}\int_0^r \rho_0(s, R)s^2 ds + \int_r^{\infty}\rho_0(s, R)s\,ds \begin{cases} -14/r \text{ for } r > R/2, \\ -28/r \text{ for } r < R/2, \end{cases} \tag{13}$$

with the monopole density

$$\rho_0(s, R) = \int_0^{\pi}\sin\theta\, d\theta \int_0^{2\pi} d\varphi\, |\Psi(N_2^+; R)|^2. \tag{14}$$

The exchange monopole potential is

$$V_{0E} = [3\rho_0(r, R)/\pi]^{1/3}. \tag{15}$$

The Coulombic quadrupole potential is

$$V_{2C}(r, R) = \tfrac{1}{2}(3\cos^2\theta - 1) \times \left[r^{-3}\int_0^r \rho_2(s, R)s^4 ds + r^2\int_r^{\infty}\rho_2(s, R)s^{-1}ds\right] - \begin{cases} 14(R/2)^2/r^3 \text{ for } r > R/2, \\ 14r^2/(R/2)^3 \text{ for } r < R/2 \end{cases}, \tag{16}$$

with the quadrupolar charge density

$$\rho_2(s, R) = \int_0^{\pi}\sin\theta\, d\theta \int_0^{2\pi} d\varphi\, \tfrac{1}{2}(3\cos^2\theta - 1)\, |\Psi(N_2^+; R)|^2. \tag{17}$$

In general, for a homonuclear diatomic with nuclear charges Z,

$$V_{JC} = Y_{J0}(\cos\theta)\frac{1}{r^{J+1}}\int_0^r \rho_J s^{J+2}ds + r^J\int_r^{\infty}\rho_J s^{1-J}ds - \begin{cases} \dfrac{Z(R/2)^J}{r^{J+1}} \text{ for } r > R/2, \\ \dfrac{Zr^J}{(R/2)^{J+1}} \text{ for } r < R/2 \end{cases}. \tag{18}$$

The exchange potential can be expressed by performing the irreducible tensorial expansion of $\rho^{1/3}$:

$$V_E = (3/\pi)^{1/3}\sum[\rho^{1/3}]_J\, Y_{J0}(\theta), \tag{19}$$

$$[\rho^{1/3}]_J = \iint \rho^{1/3}Y_{J0}(\theta)\sin\theta\, d\theta\, d\varphi. \tag{20}$$

In our calculations, we used V_{0C} and V_{0E} in finding our zero-order, one-electron wavefunctions. The obvious advantage of this procedure is that one then has in hand a set of basis functions that are eigenfunctions of orbital angular momentum ℓ^2, as well as of ℓ_z. For the evaluation of photoionization properties, we used these functions directly, assuming that ℓ is a good quantum number. For the Rydberg states, we evaluated

TABLE I. Rydberg state energies for the $^2\Sigma_g^+$ channel.

n	Zero order energies (a.u.)	$np\sigma$ first order energies (a.u.)	$np\sigma$ experimental energies[a] (a.u.)	$np\pi$ first order energies (a.u.)	$np\pi$ experimental energies[b] (a.u.)
3	−0.08013	−0.10453	−0.09725	−0.06793	−0.09727
4	−0.03968	−0.04764	···	−0.03570	−0.04603
5	−0.02396	−0.02776	−0.02609	−0.02206	−0.02702
6	−0.01608	−0.01825	−0.01733	−0.01500	−0.01776
7	−0.01154	−0.01287	···	−0.01088	−0.01257
8	−0.00869	−0.00958	−0.00915	−0.00825	−0.00935
9	−0.00678	−0.00740	···	−0.00647	−0.00724
10	−0.00544	−0.00580	···	−0.00526	−0.00573
11	−0.00446	−0.00479	···	−0.00430	−0.00468
12	−0.00372	−0.00397	···	−0.00360	−0.00385

[a]Reference 6. [b]Reference 2.

the matrix elements of V_{2C} and found the appropriate mixtures of ℓ states generated by the effect of the quadrupolar potential. Mixing could generally be evaluated by second-order perturbation theory, but in two cases, the zero-order states were so close that they had to be treated as degenerate.

Oscillator strengths for transitions to the Rydberg states were evaluated for transitions from $N_2(v''=0)$ to $N_2^*(np\sigma, np\pi, v'=0,1,2)$ ($v'=3,4$, and 5 were computed and are available on request from C. D.), and to $N_2^*(ns\sigma, nd\sigma, nd\pi, nd\delta, v'=0)$. The oscillator strength is given by

$$f_{flm} = (2m/\hbar)(E_f - E_i)\,|d_{lm}|^2, \tag{21}$$

with E_f, E_i the energies of final and initial states and d_{lm}, the dipole matrix element [Eq. (4)].

III. RESULTS: RYDBERG STATES

The energies calculated for the various Rydberg levels, relative to their ionization limits, i. e., the term values, are given in Tables I and II. Table I contains the results for the $np\sigma$ and $np\pi$ series converging to the $X^2\Sigma_g^+$ state of N_2^+, and Table II contains the $ns\sigma$, $nd\sigma$, $nd\pi$, and $nd\delta$ series converging to the $A^2\Pi_u$ state of N_2^+. Both tables are calculated for $R=R_e$ (of N_2). The zero-order energies are the eigenvalues of the electronic Hamiltonian with only V_{0C} and V_{0E} included. The first-order energies included the effect of V_{2C} as a *first*-order perturbation, so that V_{2C} makes no contribution to the ns series in Table II. Second-order corrections to the energies are small. Note that the method used here for handling exchange does not permit one to compute the singlet–triplet splitting. In Table III, we present the calculated and observed spectral lines. Note that a number of predicted lines have not yet been observed.

TABLE III. Spectral line wavelengths for certain Rydberg states.

A. Spectral line wavelengths (Å) for the $X^2\Sigma_g^+$ Rydberg states.

n	Theoretical $p\sigma$	Experimental[a] $p\sigma$	Theoretical $p\pi$	Experimental[a] $p\pi$
3	973.4	···	902.8	···
4	867.9	958.6	848.6	865.1
5	836.2	863.2	827.6	834.9
6	821.9	833.7	817.1	821.1
7	814.0	820.6	811.1	813.6
8	809.2	813.2	807.3	808.9
9	806.1	808.7	804.8	805.9
10	803.8	805.8	803.1	803.8
11	802.4	803.8	801.7	802.3
12	801.2	802.2	800.7	···

B. Spectral line wavelengths (Å) for the $A^2\Pi_u$ Rydberg states.

n	Theoretical $s\sigma$	Experimental $s\sigma$[b]	Theoretical $d\sigma$	Theoretical $d\pi$	Theoretical $d\delta$
3	986.8	946.1	998.1	935.7	787.9
4	819.5	818.6	807.7	801.5	783.4
5	783.3	783.2	778.7	776.0	768.0
6	768.0	767.8	765.9	764.4	760.0
7	760.0	759.7	758.8	758.0	755.3
8	755.3	755.4	754.6	754.0	752.3
9	752.3	752.4	751.9	751.5	750.2
10	750.3	750.3	750.0	749.7	748.8
11	748.8	748.4	748.6	748.4	747.7
12	747.8	747.3	747.6	747.4	746.9

[a]From Ref. 3. [b]From Ref. 6.

The first-order corrections to the wavefunctions were carried out in order to determine the amount of ℓ spoiling and to evaluate the effect of ℓ spoiling on the oscillator strengths and autoionization rates. For the p–f and d–g mixing in the Rydberg states with $n=8$, it was necessary to use degenerate perturbation theory, i. e., to diagonalize 2×2 matrices. In all other cases, conventional Rayleigh–Schrödinger perturbation coefficients were sufficiently accurate. In the degenerate cases the mixing was less than 3%; in all other cases the absolute values of the mixing coefficients themselves never exceeded 0.06. Hence the Rydberg states of N_2

TABLE II. Rydberg state energies for the $^2\Pi_u$ channel.

n	First order s energies (a.u.)	Experimental s energies[a] (a.u.)	Zero order d energies (a.u.)	First order $d\sigma$ energies	First order $d\pi$ energies	First order $d\delta$ energies
3	−0.15170	−0.13231	−0.09604	−0.15692	−0.12648	−0.03516
4	−0.05745	−0.05722	−0.04057	−0.04931	−0.04494	−0.03183
5	−0.03180	−0.03213	−0.02429	−0.02835	−0.02632	−0.02023
6	−0.02022	−0.02041	−0.01624	−0.01854	−0.01739	−0.01394
7	−0.01399	−0.01413	−0.01164	−0.01304	−0.01234	−0.01024
8	−0.01024	−0.01033	−0.00875	−0.00969	−0.00922	−0.00781
9	−0.00783	−0.00789	−0.00682	−0.00748	−0.00715	−0.00616
10	−0.00618	−0.00624	−0.00547	−0.00595	−0.00571	−0.00499
11	−0.00500	−0.00504	−0.00448	−0.00484	−0.00466	−0.00412
12	−0.00414	−0.00417	−0.00374	−0.00402	−0.00388	−0.00346

[a]Reference 6.

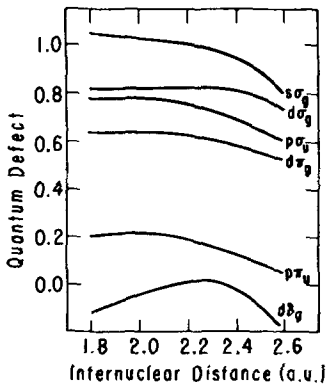

FIG. 1. Quantum defects of Rydberg states of N_2 as functions of internuclear distance. The values given here are the limits as $n \to \infty$. Quantum defects are shown for all optically allowed levels leading to the $X\,^2\Sigma_g^+$ and $A\,^2\Pi_u$ states of N_2^+; the u levels are built on the potential of the $X\,^2\Sigma_g^+$ core and the g levels are built on the potential of the $A\,^2\Pi_u$ core.

are nearly atom-like, with nearly conserved orbital angular momenta of the Rydberg electron. Ritchie,[27] on the basis of a somewhat different model, inferred that mixing would be weak for excited states arising from promotions out of the valence $p\sigma_g$ orbitals.

The computed term values and spectral line frequencies compare agreeably with the experimental values for the $p\sigma_u$, $p\pi_u$, and $s\sigma_g$ Rydberg states, where the discrepancies are about 3%, 1%, and 1%, respectively. The $p\pi_u$ levels calculated for N_2 are as satisfactory as the $p\sigma_u$ and $s\sigma_g$ levels. This is in contrast to the situation found by Berry and Nielsen[15] for H_2, where the $p\pi_u$ levels do not agree as well with experimental values as the $p\sigma_u$.

To show the dependence of the term values on internuclear distance, we have plotted the quantum defects $\mu(R)$, for six series $s\sigma_g$, $p\sigma_u$, $p\pi_u$, $d\sigma_g$, $d\pi_g$, and $d\delta_g$ in Fig. 1. Here the term values $E(n,\ell) = -1/(2n^{*2})$; the effective quantum number $n^*(n,\ell)$ is the difference between the integer n (the principal quantum number) and the quantum defect $\mu(n,l)$: $n^* = n - \mu$. Note that the quantum defects are monotonic decreasing functions of R, except for the $d\delta_g$, which exhibits a maximum. Berry and Nielsen observed similar behavior for the quantum defects in H_2.

The "vibronic" oscillator strengths have been calculated for transitions from the ground electronic state of N_2, with the initial vibrational quantum number $v'' = 0$, to Rydberg states with $n = 3$–12 and vibrational quantum numbers $v' = 0$, 1, and 2 for the $^2\Sigma_g^+$ series (f's for $v' = 3$–5 were also calculated; they are small, and decrease as v' increases) and for $n = 5$–12, $v' = 0$–3 for the $^2\Pi_u$ series. We have not applied Hönl–London factors to distribute these oscillator strengths among rotational lines within the vibrational bands. The oscillator strength is noticeably affected by quadrupole-induced configuration mixing in only the case of the $d\sigma_g$ levels; the other values are hardly changed. Table IV gives these results.

Configuration interaction does affect the distribution of $p\sigma_u$ oscillator strength among the Rydberg states, but this is largely an n-spoiling, ℓ-preserving interaction. The mixing among (n,ℓ) (n',ℓ) states is large. For $p\sigma_u$ states, the mixing coefficients for n, ℓ mixing with $(n \pm 1)\ell$ have absolute value of about 0.3; for n mixing with $n \pm 2$, the values are about 0.1. Mixing coefficients for other n' states decrease rapidly as $|n' - n|$ increases. The coefficient of the $(n-1)\,\sigma$ admixture to the predominantly $n\sigma$ state is opposite in sign to the dominant $n\sigma$ state which in turn makes the ground $\to (n-1)\sigma$ part of the dipole transition amplitude have sign opposite to the ground $\to n\sigma$ part, in the total ground $\to$ "$n\sigma$" transition amplitude. The $(n-1)\sigma$ part is quite important for the intensity of the transition, because the transition probability from ground to Rydberg states falls off fairly rapidly with increasing n. For $n < 8$, the larger parts of the oscillator strengths for "$np\sigma_u$" transitions come from the admixture of $(n-1)p\sigma_u$ basis states. Because of the opposite phase of the $(n-1)p\sigma$ and $np\sigma$ configurations in the "$np\sigma$" states, the corresponding configurational transition amplitudes have opposite sign. There is a near cancellation of the two contributions at about $n = 8$. This appears as the minimum in Fig. 2a; the Rydberg intensities rise between $n = 9$ and the ionization threshold.

We should comment on the relationship of the minimum in the oscillator strength distribution in the $np\sigma_u$ series of N_2 with the phenomenon called the "Cooper minimum."

TABLE IV. Oscillator strengths for certain Rydberg states.

A. Oscillator strengths for $(^2\Sigma_g^+)\,np$ Rydberg states.[a]

n	f for $v' = 0$	f for $v' = 1$	f for $v' = 2$
3	0.1077 (0)	0.3324 (−1)	0.3899 (−2)
	0.2980 (−3)	0.1027 (−3)	0.2575 (−4)
4	0.1911 (−1)	0.5048 (−2)	0.5733 (−2)
	0.2551 (−4)	0.1158 (−3)	0.2324 (−4)
5	0.3902 (−2)	0.9585 (−3)	0.1173 (−3)
	0.2131 (−5)	0.8551 (−4)	0.1612 (−4)
6	0.7916 (−3)	0.1491 (−3)	0.1537 (−4)
	0.2282 (−5)	0.6217 (−4)	0.1154 (−4)
7	0.6442 (−3)	0.9775 (−5)	0.1421 (−5)
	0.1135 (−5)	0.4508 (−4)	0.8288 (−5)
8	0.4499 (−6)	0.1624 (−5)	0.1763 (−6)
	0.5951 (−6)	0.3571 (−4)	0.6426 (−5)
9	0.8751 (−4)	0.3318 (−4)	0.6292 (−5)
	0.5183 (−6)	0.1963 (−4)	0.4852 (−5)
10	0.1730 (−3)	0.5695 (−4)	0.6292 (−5)
	0.5073 (−6)	0.2140 (−4)	0.3855 (−5)
11	0.1320 (−3)	0.4252 (−4)	0.5605 (−5)
	0.3836 (−6)	0.1636 (−4)	0.2854 (−5)
12	0.2649 (−3)	0.8422 (−4)	0.1051 (−4)
	0.1963 (−6)	0.1382 (−4)	0.2458 (−5)

B. Oscillator strengths for $(^2\Pi_u)\,n\ell$ Rydberg states.[a]

n	f for s states	f for $d\sigma$ states	f for $d\pi$ states	f for $d\delta$ states
5	0.2160 (−2)	0.1202 (−2)	0.3035 (−2)	0.1651 (−1)
6	0.1067 (−2)	0.3662 (−3)	0.8647 (−3)	0.4736 (−2)
7	0.6120 (−3)	0.1046 (−3)	0.3124 (−3)	0.1220 (−2)
8	0.3858 (−3)	0.2710 (−4)	0.4383 (−4)	0.2547 (−3)
9	0.2575 (−3)	0.3824 (−5)	0.1883 (−5)	0.8694 (−4)
10	0.1699 (−3)	0.3440 (−7)	0.3918 (−5)	0.7442 (−4)
11	0.1328 (−3)	0.2090 (−5)	0.1561 (−4)	0.1620 (−4)
12	0.9866 (−4)	0.2747 (−5)	0.1791 (−4)	0.1422 (−4)

[a]The upper number for each n is the $p\sigma_u$ oscillator strength and the lower the π_u. Powers of 10 are in parentheses.

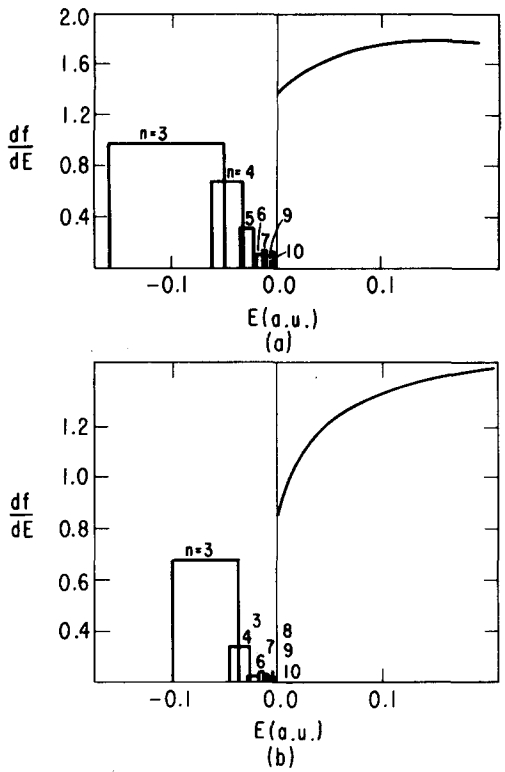

FIG. 2. Oscillator strength densities for production of $np\sigma_u$ and $np\pi_u$ Rydberg levels and for photoionization of N_2 to N_2^+ $(X\,^2\Sigma_g^+) + e$: (a) $p\sigma_u$ channels; (b) $p\pi_u$ channels.

The latter is a minimum in the oscillator strength distribution coming from a change of sign in the radial factor of the dipole matrix element for a one-electron transition as the energy of the final state varies.[29] The N_2 series minimum arises from a change of sign in the transition amplitude, but from the variation in configuration mixing with final-state energy. The change of sign in the Cooper process occurs because of a one-electron property: a node of the final one-electron function moves inward through the dominant lobe of the initial orbital, as the transition energy increases. The two sorts of minima produce the same effect on the total cross section, but one is based on a one-electron property and the other on correlation—or at least so it seems, stemming as it does from configuration interaction. We must tread cautiously in applying this interpretation to our calculation of N_2 itself because the CI we have done is not based on Hartree–Fock configurational functions, and involves only configurations that differ in the orbital assignment of a single electron. We, therefore, cannot argue that the configuration mixing in *our* calculations on N_2 is entirely or even predominantly coming from electron correlation. Nevertheless, the results show us that a second mechanism can exist, different from the cause of the Cooper minimum, that should also give rise to minima in oscillator strength distributions. Transition amplitudes and CI coefficients of a Rydberg series can, in general, be expected to vary smoothly with the upper-state principal quantum number. We can therefore expect a phenomenon to occur in which truly correlative CI causes effects such as we find in the $np\sigma_u$ series of N_2: that a lower configuration contributes a small share to the total wavefunction but a large share to the oscillator strength; that the two main contributions to the transition amplitude may have opposite sign, and, when this is the case, there is some critical energy below which one configuration's transition amplitude dominates the total amplitude and sign, and above which, the other configuration dominates. This change, which we can call a change in "transition dominance," is clearly not directly related to which configuration dominates the composition of a state function i. e., to the "configuration dominance" of a state. It may well be useful to distinguish generally between transition dominance and configuration dominance, as the role of configuration interaction becomes better understood in optical processes, impact excitation and radiationless transitions.

Configuration mixing among the $np\pi_u$ Rydberg basis functions is less than for the $np\sigma_u$'s. Moreover, the coefficients for $n' < n$ are positive, causing an increase in the $np\pi_u$ amplitudes, rather than a cancellation of the kind we find for the $np\sigma_u$ levels.

Among the transitions converging to the $^2\Pi_u$ state of N_2^+, the $d\sigma_g$ and $d\pi_g$ series behave like the $p\sigma_u$ series, with destructive interference among neighboring configurations, creating minima in f as a function of n and, for higher n, pushing oscillator strength upward into the continuum, in a kind of sequence of nudges. The $s\sigma_g$ and $d\delta_g$ states, on the other hand, behave like the $p\pi_u$ states and keep the Rydberg oscillator strength within the family of bound states. As Table IVb shows, f for the $s\sigma_g$ and $d\delta_g$ series decrease monotonically. Plots of the sort used by Fano and Cooper[29] to display the oscillator strength *per unit energy*, or the average oscillator strength density, are shown in Figs. 2, 3, and 4.

The oscillator strength distributions of Figs. 2, 3, and 4 indicate sharp changes in these distributions in the vicinity of the ionization thresholds. This is in contrast to the normal expectation of how oscillator strength behaves, of course. There are two factors that appear to be the cause of this behavior, one physical and the other, an artifact of the calculation. The physical contribution from the occurrence of zeros in dipole transition amplitude is discussed above. The computational artifact arises because the bound-state oscillator strengths and the continuum oscillator strengths were

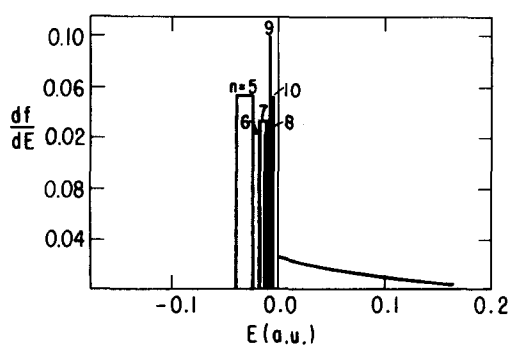

FIG. 3. Oscillator strength density for production of $ns\sigma_g$ Rydberg levels and for photoionization of N_2 to $N_2^+(A\,^2\Pi_u) + e(ks\sigma_g)$.

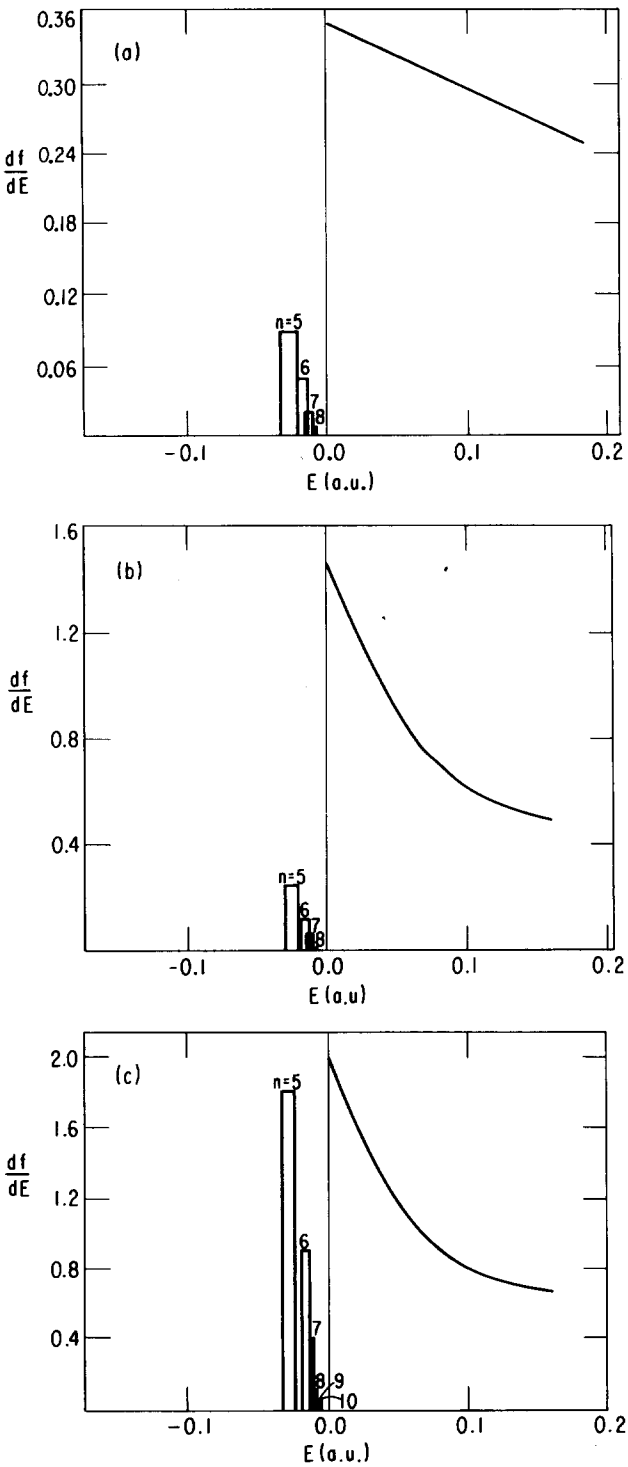

FIG. 4. Oscillator strength densities for production of (a) $nd\sigma_g$, (b) $nd\pi_g$, and (c) $nd\delta_g$ Rydberg levels of N_2 and for photoionization to the corresponding partial wave final states built on $N_2^+(^2\Pi_g)$.

not evaluated with the same kind of final-state wavefunction. The bound Rydberg states were represented by wave functions with CI. The continuum one-electron functions were single partial-wave Coulomb functions, phase-shifted by the short-range potential of the N_2^+ core and orthogonalized to the core orbitals, but the final-state configurational functions were not allowed to interact.

We should point out that theoretical calculations of Rydberg states of N_2 have been carried out previously, particularly by Lefebvre-Brion and Moser,[30] by Duncan,[31] and by Duncan and Damiani.[32] These calculations were directed toward identification of the various Rydberg series of N_2, and were not concerned with the intensities of the transitions. They were computed with Slater-type basis functions for the Rydberg electrons, and with somewhat simpler core functions than those we used. In the sense that these calculations were earlier, simpler, and aimed at interpreting grosser aspects of the Rydberg levels than our own calculations, there is little point in trying to draw detailed comparisons with the present results. Where comparisons are possible, (apart from the $^1\Pi_u$, 3s Rydberg level), the discrepancies between our calculations and experimental levels are one-half to one-third of those of the earlier computations.

IV. RESULTS: CONTINUUM

The hypothetical photoionization cross sections for direct transitions to the continuum partial waves are given, in effect, by the smooth curves of Figs. 2–4 above the ionization thresholds. These are, as we indicated previously, transition probabilities integrated over internuclear distance as well as over electronic coordinates. To interpret the ionization cross sections, we should go back a step, to examine the dependence of the transition amplitudes on R. The $3\sigma_g \rightarrow k\sigma_u$ process has a large amplitude and, as Fig. 5 indicates, has a strong dependence on R. The transition to the $k\pi_u$ states is small by comparison and varies much less with R—although it does have a zero when $R \cong 2.24$ a.u., as seen in the figure. While Fig. 5 shows the behavior of the amplitudes for only the photon energy of 0.2073 a.u. (the energy of the He 584 Å line), the same general behavior occurs over the energy range of this study. The transition amplitudes from the $1\pi_u \rightarrow k\pi_g$, the slope is comparable to that for the $3\sigma \rightarrow k\pi_u$ transition. For the $k\sigma_g$ (whether s- or d-like) and the $k\delta_g$ final states, the R dependence is still less. In general, matrix elements for transitions to $p\sigma_u$, $p\pi_u$, and $s\sigma_g$ orbitals increase with R, while those for transitions to d waves decrease with R, in the interval of R that we examined.

The total photoionization cross sections for production of $N_2^+(X^2\Sigma_g^+)$ and $N_2^+(^2\Pi_u)$ are given in Table V. This table includes our calculated values, the computed values obtained by Schneider and Berry,[14] by Ellison

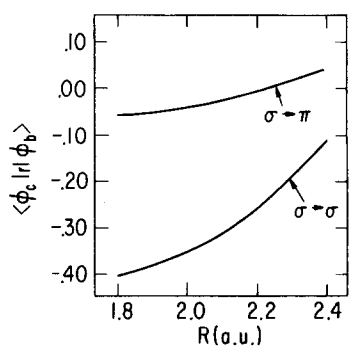

FIG. 5. Electric dipole transition amplitudes for $3\sigma_g \rightarrow k\sigma_u$ and $3\sigma_g \rightarrow k\pi_u$ ionization processes, as functions of internuclear distance. The curves shown are for an electron energy of 0.2073 a.u. (5.64 eV) or for photons of energy 21.2 eV, corresponding to the He I 584 Å resonance line. The core is $N_2^+(^2\Sigma_g^+)$.

TABLE V. Cross sections for photoionization of N_2 (bohr^2).

Photoelectron energy (a.u.)	Photon wave length (Å)	Final state of ion	σ (this work)	σ (other calculations)	σ_{exp} (Ref. 9)[a]	σ_{exp} (Ref. 10)
0.00005	795.8	$^2\Sigma_g^+$	0.0879	0.1594[b]; 0.47[c]	0.1436	···
0.001	794.5	$^2\Sigma_g^+$	0.0893	···	0.1942	···
0.01	782.2	$^2\Sigma_g^+$	0.0907	···	0.3657	···
0.0467	747.7	$^2\Sigma_g^+$	0.0953	0.1482[b]; 0.39[c]; 0.012[d]	0.6649	···
0.10	677.5	$^2\Sigma_g^+$	0.0999	0.37[c]	···	0.225
0.15	630.6	$^2\Sigma_g^+$	0.1021	0.36[c]	···	0.31
0.2073	584.3	$^2\Sigma_g^+$	0.1021	0.0621[b]; 0.38[c]; 0.039[d]	···	0.31
0.9261	304.0	$^2\Sigma_g^+$	0.0635	···	···	···
0.0057	735.9	$^2\Pi_u$	0.4785	0.1172[b]	···	···
0.059	677.5	$^2\Pi_u$	0.2893	0.728[c]	···	0.55
0.109	630.6	$^2\Pi_u$	0.2130	0.846[c]	···	0.44
0.1663	584.3	$^2\Pi_u$	0.1846	0.1222[b]; 0.983[c]; 0.141[d]	···	0.45
0.8851	304.0	$^2\Pi_u$	0.0472	···	···	···

[a]At 677.5 Å, Ref. 9 gives a total cross section of 0.6317, with which our combined X and A cross sections can be compared; we obtain $0.3892a_0^2$.
[b]Reference 14.
[c]Estimated from the curves of Ref. 35, Fig. 2, which are constructed to show the distribution of oscillator strengths among vibrational bands.
[d]Reference 34.

et al.,[33,34] and by Tuckwell[35] from simpler theoretical models, the experimental cross section reported by Cook and Ogawa,[9] and the newly measured set of experimental values reported to us by Samson.[10] Theoretical values and experimental values are plotted in Fig. 6. The agreement is within about a factor of 2, and the shape of the $^2\Sigma_g^+$ cross section is essentially flat, according to theory and experiment. The experimental $^2\Pi_u$ cross section exhibits a rise and fall quite different from the declining curve we compute. The most obvious ways to try to improve the agreement, in the probable order of their importance, are (1) inclusion of partial wave mixing in the final continuum functions; (2) replacement of the local approximation to the exchange terms with the true exchange interaction; and (3) inclusion of polarization in the final state interactions, either as a simple static term or in a more exact way.

The calculations of Ellison *et al.* are based on a plane wave representation of the continuum functions, orthogonalized to the occupied orbitals.[33,34] This approach has strong appeal because of its computational convenience. However, we see that it is not reliable, as Tables V and VI indicate, for representing processes in the regions of ionization thresholds. This result is not unexpected, and appropriate cautions were given in the original presentation of the results. The low-energy Coulomb functions change shape too much over the range of atomic distances to be well represented by plane waves, even by plane waves in which extra nodes have been introduced by orthogonalization.

Tuckwell's calculations of the photoionization cross sections are based on Slater-type exponential approximations to the bound orbitals. The continuum functions are based on the bicentric Coulomb potential of the type used by Flannery and Öpik,[36] with a phase shift based on a molecular extension of the quantum defect method.[37] The continuum functions were not orthogonalized to the core functions. Tuckwell's results are almost all higher than those calculated by other methods. In our experience, orthogonalization of continuum functions to the appropriate core orbitals nearly always

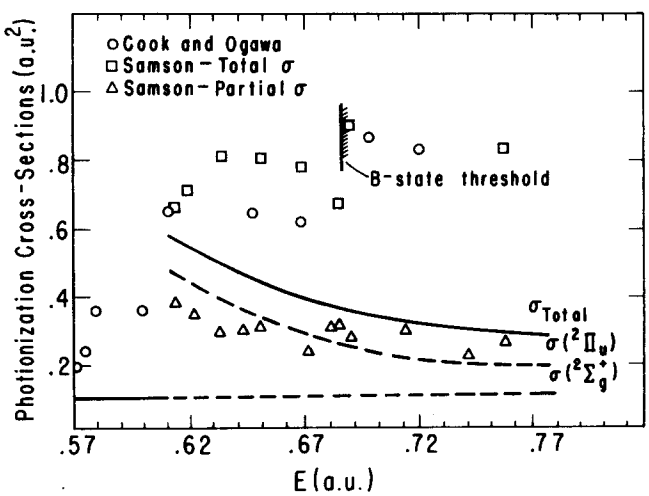

FIG. 6. Photoionization cross sections of N_2 as functions of energy. Solid curve: our total (theoretical); lower dashed curve: theoretical cross section for production of $N_2^+(X\,^2\Sigma_g^+)$; upper dashed curve: theoretical cross section for production of $N_2^+(A\,^2\Pi_u)$; circles: Ref. 9, total cross section; squares: Ref. 10, total cross section; triangles: Ref. 10, cross section for production of $N_2^+(X\,^2\Sigma_g^+)$.

reduces the magnitude of transition amplitudes. If the computationally attractive bicentric quantum defect method were to be pursued further, it would be well worth testing the effect of orthogonalization.

Another characteristic of bound-free transtions was evaluated, the photoelectron angular distribution, or differential cross section. Experimental values of the asymmetry parameter β have been obtained for N_2 at energies corresponding to the resonance lines of He I and Ne I, 584.3 and 747.7 Å, respectively. For the $^2\Sigma_g^+ \times (v' = 0)$ channel, the experimental values are 0.5 ± 0.1,[11] 0.3,[38] and 0.9[39] at 584.3 Å and 1.2 ± 0.2 at 747.7 Å. For the $^2\Pi_u$ final channel, $\beta = 0.3 \pm 0.1$[11,39] and 0.12[38] at 21.22 eV. (The first set of observations for N_2 had given a value of β near zero.[40]) Our values are 1.01, 0.99, and 0.49, in that order, so that the agreement is tolerable except at 584.3 Å. Experimental and theoretical values of β for both final states of N_2^+ are given in Table VI.

The variation of the transition dipole moments with R can lead to a variation of β or β' with vibrational quantum number of the final ion. We find such variation with v' in the $N_2^+(^2\Sigma_g^+)$ state, but not so marked as in the observation reported by Carlson and Jonas.[11] Figure 7 gives the calculated and experimental curves of $I(\theta, v' = 1)/I(\theta, v' = 0)$ for $^2\Sigma_g^+$ production. For the $^2\Pi_u$ state, our theoretical values of β for $v' = 0$ and $v' = 1$ are identical within the limits of computational accuracy. This is in agreement with the observations of Carlson and Jonas; no dependence of β on v' was found in the production of $N_2^+(^2\Pi_u)$. It would be useful to have experimental values of β or β' at several energies, to compare with our results. Unfortunately the Ne II resonance line and the He II ($Ly\alpha$) lines are less than ideal for this purpose. The Ne II line is in a region beset by autoionization. The He II line is outside the autoionization region but is at such high energy that contributions to β from higher partial waves may be important.

TABLE VI. β as a function of energy.

Energy of photoionized electron (a.u.)	Channel	β_{theor}	β_{exp}
0.00005	$^2\Sigma_g^+$	0.96; 0.39[b]	···
0.001	$^2\Sigma_g^+$	0.96	···
0.01	$^2\Sigma_g^+$	0.97	···
0.0467	$^2\Sigma_g^+$	0.99; 0.31[b]	1.22 ± 0.2[a]; 1.93[c]
0.1	$^2\Sigma_g^+$	1.01	···
0.15	$^2\Sigma_g^+$	1.02	···
0.2073	$^2\Sigma_g^+$	1.01; 0.68[b]	0.5 ± 0.1[a]; 1.91[c]; 0.9[d]
0.9261	$^2\Sigma_g^+$	0.81	1.2[d]
0.0057	$^2\Pi_u$	0.74	···
0.0590	$^2\Pi_u$	0.63	···
0.109	$^2\Pi_u$	0.54	···
0.1663	$^2\Pi_u$	0.49	0.3 ± 0.1[a]; 0.720[c]; 0.3[d]
0.8851	$^2\Pi_u$	0.004	1.0[d]

[a]Reference 11. [c]Reference 35.
[b]Reference 14. [d]Reference 39.

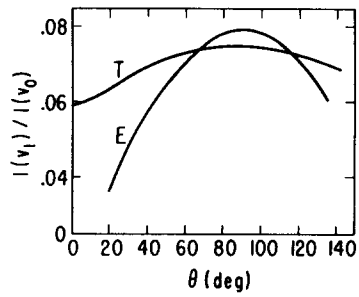

FIG. 7. Experimental (E) and theoretical (T) curves of the ratio of intensity of photoelectrons for production of the $v' = 1$ and $v' = 0$ states of N_2^+, as a function of the angle θ of the outgoing photoelectron momentum with respect to the axis of polarization of the incident light. (E curve from Ref. 11).

ACKNOWLEDGMENTS

We would like to thank Dr. J. A. R. Samson and Dr. P. K. Carroll for communicating results to us prior to publication, and Dr. F. O. Ellison for his comments on the manuscript. This research was supported by the National Science Foundation.

*Present address: Department of Chemistry, University of Toronto, Toronto, Canada.

[1]R. E. Worley and F. A. Jenkins, Phys. Rev. 54, 305 (1938).
[2]P. K. Carroll and K. Yoshino, J. Chem. Phys. 47, 3073 (1967).
[3]P. K. Carroll and K. Yoshino, J. Phys. B 5, 1614 (1972).
[4]J. W. Ledbetter, Jr., J. Mol. Spectrosc. 42, 100 (1972).
[5]R. E. Worley, Phys. Rev. 64, 207 (1943).
[6]M. Ogawa and Y. Tanaka, Can. J. Phys. 40, 1593 (1962).
[7]M. Ogawa, Can. J. Phys. 42, 1087 (1964).
[8]G. R. Cook and P. H. Metzger, J. Chem. Phys. 41, 321 (1964).
[9]G. R. Cook and M. Ogawa, Can. J. Phys. 43, 256 (1965).
[10]J. A. R. Samson (private communication, December 1974).
[11]T. A. Carlson and A. E. Jonas, J. Chem. Phys. 55, 4913 (1971).
[12]J. Berkowitz and W. A. Chupka, J. Chem. Phys. 51, 2341 (1969).
[13]P. Dehmer and W. A. Chupka (private communication, 1974).
[14]B. Schneider and R. S. Berry, Phys. Rev. 182, 141 (1969).
[15]R. S. Berry and S. E. Nielsen, J. Chem. Phys. 49, 116 (1968).
[16]B. Ritchie, J. Chem. Phys. 60, 898 (1974).
[17]R. W. Ditchburn and U. Öpik, in *Atomic and Molecular Processes*, edited by D. R. Bates (Academic, New York, 1962), p. 23.
[18]C. N. Yang, Phys. Rev. 74, 764 (1968).
[19]J. Cooper and R. N. Zare, in *Atomic Collision Processes*, edited by S. Geltman, K. Manhanthappa, and W. Brittin (Gordon and Breach, New York, 1969), p. 243.
[20]J. C. Tully, R. S. Berry, and B. J. Dalton, Phys. Rev. 176, 95 (1968).
[21]F. R. Gilmore, J. Quant. Spectrosc. Radiat. Transfer 5, 369 (1965).
[22]T. W. Cooley, Math. Comp. 15, 363 (1961).
[23]J. C. Slater, Phys. Rev. 81, 385 (1951).

[24]B. Y. Tong and L. T. Sham, Phys. Rev. 144, 1 (1966).
[25]R. S. Berry and S. E. Nielsen, Phys. Rev. A 1, 383 (1970).
[26]B. Ritchie, J. Chem. Phys. 61, 3279, 3291 (1974).
[27]B. Ritchie, "Theoretical Studies in Photoelectron Spectroscopy, IV." (in press).
[28]P. Cade, K. D. Sales, and A. C. Wahl, J. Chem. Phys. 44, 1973 (1966)
[29]U. Fano and J. W. Cooper, Rev. Mod. Phys. 40, 441 (1968).
[30]H. Lefebvre-Brion and C. Moser, J. Chem. Phys. 43, 1394 (1965).
[31]A. B. F. Duncan, J. Chem. Phys. 42, 2453 (1965).
[32]A. B. F. Duncan and A. Damiani, J. Chem. Phys. 45, 1245 (1966).
[33]F. O. Ellison, J. Chem. Phys. 61, 507 (1974); 62, 4287 (1975).
[34]J. W. Rabalais, T. P. Debies, J. L. Berbosky, J.-T. J. Huang, and F. O. Ellison, J. Chem. Phys. 61, 516, 529 (1974); 62, 4287 (1975).
[35]H. Tuckwell, J. Phys. B 3, 293 (1970).
[36]M. R. Flannery and U. Öpik, Proc. Phys. Soc. London 86, 491 (1965).
[37]M. Weinberg, R. S. Berry, and J. C. Tully, J. Chem. Phys. 49, 122 (1968).
[38]J. A. R. Samson, Philos. Trans. R. Soc. London Ser. A 268, 141 (1970).
[39]M. Nakamura, Y. Iida, and K. Kondo, Studies of Atomic Collisions and Related Topics in Japan, Prog. Rept. 2, March 1974, p. 100.
[40]J. Berkowitz, H. Ehrhardt, and T. Tekaat, Z. Phys. 200, 69 (1967).